Fantasia3D: Disentangling Geometry and Appearance for High-quality Text-to-3D Content Creation

Rui Chen*, Yongwei Chen*, Ningxin Jiao, Kui Jia†
South China University of Technology

Abstract

Automatic 3D content creation has achieved rapid progress recently due to the availability of pre-trained, large language models and image diffusion models, forming the emerging topic of text-to-3D content creation. Existing text-to-3D methods commonly use implicit scene representations, which couple the geometry and appearance via volume rendering and are suboptimal in terms of recovering finer geometries and achieving photorealistic rendering; consequently, they are less effective for generating high-quality 3D assets. In this work, we propose a new method of Fantasia3D for high-quality text-to-3D content creation. Key to Fantasia3D is the disentangled modeling and learning of geometry and appearance. For geometry learning, we rely on a hybrid scene representation, and propose to encode surface normal extracted from the representation as the input of the image diffusion model. For appearance modeling, we introduce the spatially varying bidirectional reflectance distribution function (BRDF) into the text-to-3D task, and learn the surface material for photorealistic rendering of the generated surface. Our disentangled framework is more compatible with popular graphics engines, supporting relighting, editing, and physical simulation of the generated 3D assets. We conduct thorough experiments that show the advantages of our method over existing ones under different text-to-3D task settings. Project page and source codes: `https://fantasia3d.github.io/`.

1. Introduction

Automatic 3D content creation [43, 18, 33, 44] powered by large language models has drawn significant attention recently, due to its convenience to entertaining and gaming industries, virtual/augmented reality, and robotic applications. The traditional process of creating 3D assets typically involves multiple, labor-intensive stages, including geometry modeling, shape baking, UV mapping, material creation, and texturing, as described in [15], where different software tools and the expertise of skilled artists are often required. Imperfections would also accumulate across these stages, resulting in low-quality 3D assets. It is thus desirable to automate such a process, and ideally to generate high-quality 3D assets that have geometrically fair surfaces, rich materials and textures, and support photorealistic rendering under arbitrary views.

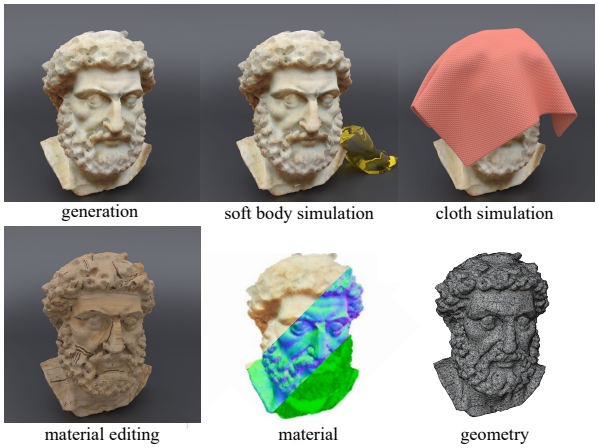

Figure 1. Provided with a textual description of "a highly detailed stone bust of Theodoros Kolokotronis", our method produces high-quality geometry as well as disentangled materials, and enables photorealistic rendering.

In this work, we focus on automatic 3D content creation given text prompts encoded by large language models, i.e., the text-to-3D tasks [18, 33]. Text-to-3D is inspired by the tremendous success of text-to-image research [34, 36, 30, 35]. To enable 3D generation, most existing methods [33, 23] rely on the implicit scene modeling of Neural Radiance Field (NeRF) [25, 4, 27], and learn the NeRFs by back-propagating the supervision signals from image diffusion models. However, NeRF modeling is less effective for surface recovery [43, 46], since it couples the learning of surface geometry with that of pixel colors via volume rendering. Consequently, 3D creation based on

*Equal contribution.
†Corresponding author.

NeRF modeling is less effective for recovery of both the fine surface and its material and texture. In the meanwhile, explicit and hybrid scene representations [43, 46, 38] are proposed to improve over NeRF by modeling the surface explicitly and performing view synthesis via surface rendering.

In this work, we are motivated to use 3D scene representations that are more amenable to the generation of high-quality 3D assets given text prompts. We present an automatic text-to-3D method called Fantasia3D. Key to Fantasia3D is a disentangled learning of geometry and appearance models, such that both a fine surface and a rich material/texture can be generated. To enable such a disentangled learning, we use the hybrid scene representation of DMTET [38], which maintains a deformable tetrahedral grid and a differentiable mesh extraction layer; deformation can thus be learned through the layer to explicitly control the shape generation. For geometry learning, we technically propose to encode a rendered normal map, and use shape encoding of the normal as the input of a pre-trained, image diffusion model; this is in contrast different from existing methods that commonly encode rendered color images. For appearance modeling, we introduce, for the first time, the spatially varying Bidirectional Reflectance Distribution Function (BRDF) into the text-to-3D task, thus enabling material learning that supports photorealistic rendering of the learned surface. We implement the geometry model and the BRDF appearance model as simple MLPs. Both models are learned through the pre-trained image diffusion model, using a loss of Score Distillation Sampling (SDS) [33]. We use the pre-trained stable diffusion [35, 40] as the image generation model in this work.

We note that except for text prompts, our method can also be triggered with additional inputs of users' preferences, such as a customized 3D shape or a generic 3D shape of a certain object category; this is flexible for users to better control what content is to be generated. In addition, given the disentangled generation of geometry and appearance, it is convenient for our method to support relighting, editing, and physical simulation of the generated 3D assets. We conduct thorough experiments to verify the efficacy of our proposed methods. Results show that our proposed Fantasia3D outperforms existing methods for high-quality and diverse 3D content creation. We summarize our technical contributions as follows.

- We propose a novel method, termed Fantasia3D, for high-quality text-to-3D content creation. Our method disentangles the modeling and learning of geometry and appearance, and thus enables both a fine recovery of geometry and photorealistc rendering of per-view images.
- For geometry learning, we use a hybrid representation of DMTET, which supports learning surface deformation via a differentiable mesh extraction; we propose to render and encode the surface normal extracted from DMTET as the input of the pre-trained image diffusion model, which enables more subtle control of shape generation.
- For appearance modeling, to the best of our knowledge, we are the first to introduce the full BRDF learning into text-to-3D content creation, facilitated by our proposed geometry-appearance disentangled framework. BRDF modeling promises high-quality 3D generation via photorealistic rendering.

2. Related work

Text-to-3D content creation. Motivated by the desire to generate high-quality 3D content from simple semantics such as text prompts, text-to-3D has drawn considerable attention in recent years [33, 13, 18]. Existing methods either use pre-trained 2D text-to-image models [35, 3, 36], together with score distillation sampling [33], to generate 3D geometries [18] or synthesize novel views [33], or train a text-conditioned 3D generative model from scratch [39, 49, 17, 29]. These methods generate 3D geometries with little exploration of generating high-quality lighting and surface materials. On the other hand, TANGO [8] is able to generate high-quality surface materials given text prompts; unfortunately, the method requires as input a 3D surface mesh. Our proposed method addresses the shortcomings of the above methods, and is able to generate both high-quality surface geometries and their corresponding materials, both of which are crucial for photorealistic rendering of the generated 3D content. Our method thus, for the first time, closes the loop of object-level text-to-3D content creation.

Surface material estimation. The estimation of surface materials is a long-standing challenge in computer vision and graphics research. Earlier methods [2, 45] focus on recovering physically based materials under known lighting conditions, whose usefulness is, however, limited in real-world scenarios. Subsequent methods [12, 11, 5, 1] try to estimate materials under natural lighting conditions, assuming the availability of complete geometry information. More recently, the joint reconstruction of geometry and materials is proposed given calibrated multi-view images [6, 7, 19, 48]. Alternative to these methods, we explore the novel creation of surface materials and geometries from trained language models.

3. Preliminary

In this section, we present a few preliminaries that are necessary for presenting our proposed method in Section 4.

Figure 2. **Results of our method.** The upper portion of this figure showcases the generation results obtained from solely text prompts. The lower portion showcases user-guided generation results given guiding meshes with the corresponding textual descriptions.

3.1. Score distillation sampling

DreamFusion [33] presents a method that optimizes 3D scene parameters and synthesizes novel views from textual descriptions, by employing a pre-trained 2D diffusion model. The scene is represented as a differentiable image parameterization [26], where a differentiable generator g

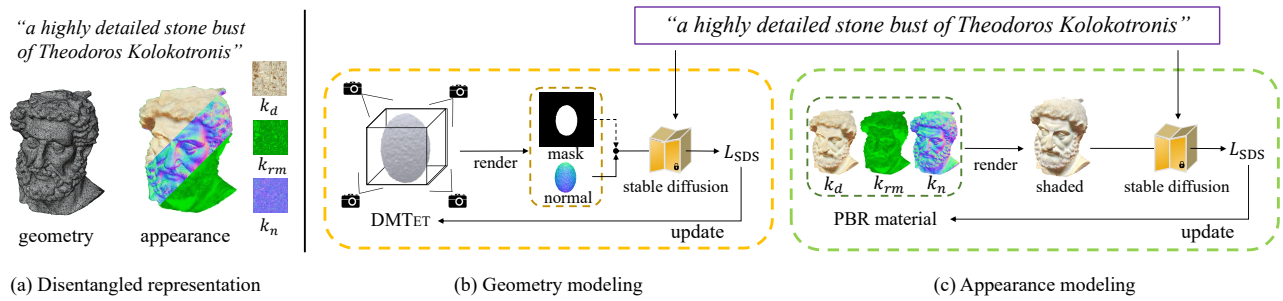

(a) Disentangled representation (b) Geometry modeling (c) Appearance modeling

Figure 3. **Overview of our method.** Our method can generate disentangled geometry and appearance given a text prompt (cf. figure (a)), which are produced by (b) geometry modeling and (c) appearance modeling, respectively. (b) We employ DMTET as our 3D geometry representation, which is initialized as a 3D ellipsoid here. To optimize the parameters of DMTET, we render the normal map (and the object mask in the early training phase) of the extracted mesh from DMTet as the shape encoding of stable diffusion [35, 40]. (c) For appearance modeling, we introduce the spatially-varying Bidirectional Reflectance Distribution Function (BRDF) modeling into text-to-3D generation, and learn to predict three components (namely, k_d, k_{rm}, and k_n) of the appearance. Both geometry and appearance modeling are supervised by Score Distillation Sampling (SDS) loss [33].

renders 2D images $x = g(\theta)$ from a modified Mip-NeRF [4] parameterized as θ. DreamFusion leverages a diffusion model ϕ (Imagen [36] in this instance) to provide a score function $\hat{\epsilon}_\phi(x_t; y, t)$, which predicts the sampled noise ϵ given the noisy image x_t, text-embedding y, and noise level t. This score function guides the direction of the gradient for updating the scene parameters θ, and the gradient is calculated by Score Distillation Sampling (SDS):

$$\bigtriangledown_\theta \mathcal{L}_{\text{SDS}}(\phi, x) = \mathbb{E}_{t,\epsilon}\left[w(t)(\hat{\epsilon}_\phi(x_t; y, t) - \epsilon)\frac{\partial x}{\partial \theta}\right], \quad (1)$$

while $w(t)$ is a weighting function. Since Imagen is not publicly accessible, in this work, we use the released latent space diffusion model of Stable Diffusion [35, 40] as our guidance model, and revise the SDS loss (1) accordingly. Details are given in Section 4.2.

3.2. DMTET

Implicit surface representations [25, 31, 22] are popularly used in novel view synthesis and 3D reconstruction, due to their capabilities to represent complex scenes. However, surfaces of lower quality may be obtained [28] by extracting explicit meshes from these implicit representations using marching cubes [20]. Instead, Shen et al. [38] propose a hybrid representation, termed DMTET, that has two key features, i.e., a deformable tetrahedral grid and a differentiable Marching Tetrahedral (MT) layer. The deformable tetrahedral grid (V_T, T) has vertices V_T in the tetrahedral grid T. For each vertex $v_i \in V_T$, the proposed method predicts the Signed Distance Function (SDF) value $s(v_i)$ and a position offset $\triangle v_i$ by:

$$(s(v_i), \triangle v_i) = \Psi(v_i; \psi), \quad (2)$$

where ψ is the parameters of a network Ψ, enabling the extraction of explicit meshes through MT layer during each iteration of training. In this work, We use DMTET as our geometry representation and render the mesh extracted from MT layer iteratively by a differentiable renderer[16, 28].

4. The Proposed Method

In this section, we present our proposed method of Fantasia3D for high-quality text-to-3D object generation, by disentangling the modeling and learning of geometry and appearance. For geometry modeling, we rely on the hybrid surface representation of DMTET, and parameterize the 3D geometry as an MLP Ψ that learns to predict the SDF value and position offset for each vertex in the deformable tetrahedral grid of DMTET; in contrast to previous methods, we propose to use the rendered normal map (and the object mask in the early training phase) of the extracted mesh from DMTET as the input of shape encoding. For appearance modeling, we introduce, for the first time, the full Bidirectional Reflectance Distribution Function (BRDF) modeling into text-to-3D generation, and learn an MLP Γ that predicts parameters of surface material and supports high-quality 3D generation via photorealistic rendering. Given the disentangled modeling of Ψ and Γ, the whole pipeline is learned with SDS supervision, and the gradients are back-propagated through the pre-trained stable diffusion model. Our pipeline is initialized either as a 3D ellipsoid or as a customized 3D model provided by users. Fig. 3 gives an illustration of our proposed method. In contrast, previous methods couple the geometry and appearance learning, and are suboptimal in terms of leveraging the powerful pre-trained 2D image diffusion models via SDS loss. Details of the proposed Fantasia3D are presented as follows.

4.1. DMTET initialization

We adopt DMTET as our 3D scene representation, which is parameterized as the MLP network Ψ. For each vertex $v_i \in V_T$ of the tetrahedral grid (V_T, T), Ψ is trained to predict the SDF value $s(v_i)$ and the deformation offset $\triangle v_i$. A triangular mesh can be extracted from (V_T, T) using the MT layer, whose procedure is also differentiable w.r.t. the parameters of Ψ. We initialize DMTET either as a 3D ellipsoid or as a customized 3D model provided by users; the latter choice is useful when the text-to-3D task is to be conditioned on users' preferences. In either case, we initialize Ψ by the following fitting procedure. We sample a point set $\{p_i \in \mathbb{R}^3\}$ whose points are in close proximity to the initialized 3D ellipsoid or customized model, and compute their SDF values, resulting in $\{SDF(p_i)\}$; we use the following loss to optimize the parameters ψ of Ψ:

$$\mathcal{L}_{\text{SDF}} = \sum_{p_i \in P} \|s(p_i; \psi) - SDF(p_i)\|_2^2 . \tag{3}$$

4.2. Geometry modeling

Previous text-to-3D methods [33, 13] commonly use NeRF [25, 4] as the implicit scene representation, which couples the geometry with color/appearance and use volume rendering for view synthesis. Since NeRF modeling is less effective for surface reconstruction [43, 46], these methods are consequently less effective to generate high-quality 3D surfaces by back-propagating the supervision of SDS loss through pre-trained text-to-image models. As a remedy, the method [18] uses a second stage of the refined generation that is based on scene modeling of explicit surfaces.

In this work, we propose to decouple the generation of geometry from that of appearance, based on the hybrid scene representation of DMTET, which enables photorealistic surface rendering to make better use of the powerful pre-trained text-to-image models. More specifically, given the current DMTET with MLP parameters ψ, we generate a normal map n, together with an object mask o, as:

$$(n, o) = g_n(\psi, c), \tag{4}$$

where g_n is a differentiable render (*e.g.*, nvidiffrast [16]), and c is a sampled camera pose. We randomly sample the camera poses in the spherical coordinate system to ensure that the camera poses are distributed uniformly on the sphere. We propose to use the generated n (and o) as the input of shape encoding to connect with stable diffusion. To update ψ, we again employ SDS loss that computes the gradient w.r.t. ψ as:

$$\nabla_\psi \mathcal{L}_{\text{SDS}}(\phi, \tilde{n}) = \mathbb{E}\left[w(t)(\hat{\epsilon}_\phi(z_t^{\tilde{n}}; y, t) - \epsilon) \frac{\partial \tilde{n}}{\partial \psi} \frac{\partial z^{\tilde{n}}}{\partial \tilde{n}} \right], \tag{5}$$

Figure 4. Three components of the material model, namely the diffuse term k_d, the roughness and metallic term k_{rm}, and the normal variation term k_n.

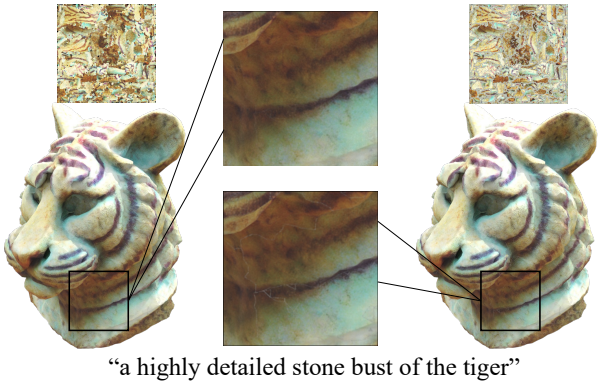

Figure 5. A comparison of UV edge padding (cf. the left column) and original texturing (cf. the right column). UV edge padding removes the white seams that appear in the right rendering.

where ϕ parameterizes the pre-trained stable diffusion model, $\tilde{n}$ denotes concatenation of the normal n with the mask o, $z^{\tilde{n}}$ is the latent code of $\tilde{n}$ via shape encoding, $\hat{\epsilon}_\phi(z_t^{\tilde{n}}; y, t)$ is the predicted noise given text embedding y and noise level t, and ϵ is the noise added in $z_t^{\tilde{n}}$. In practice, we utilize a coarse-to-fine strategy to model the geometry. During the early phase of training, we use the downsampled $\tilde{n}$ as the latent code, which is inspired by [23], to rapidly update Ψ and attain a coarse shape. However, a domain gap exists between $\tilde{n}$ and the latent space data distribution learned by the VAE encoder in the stable diffusion, which may lead to a mismatch of the generated geometry from the textual description. To mitigate this discrepancy, we implement a data augmentation technique by introducing random rotations to $\tilde{n}$. Our experimental observations reveal that this technique enhances the alignment between the generated geometry and the provided textual description. In the later phase of training, aiming to capture finer geometric details with greater precision, we encode the high-resolution normal n (without the mask o) to derive z^n, using the pre-trained image encoder in stable diffusion.

4.3. Appearance modeling

Given a learned DMTET with geometry parameters ψ, we aim for photorealistic surface rendering to better leverage the powerful image diffusion model. This is achieved by introducing into text-to-3D generation the Physically-Based Rendering (PBR) material model. As illustrated in Fig. 4, the material model we use [21] comprises three components, namely the diffuse term $k_d \in \mathbb{R}^3$, the roughness and metallic term $k_{rm} \in \mathbb{R}^2$, and the normal variation term $k_n \in \mathbb{R}^3$. The k_d term denotes the diffuse value, while the k_{rm} term encompasses the roughness r and metalness m; the roughness r serves as a metric for measuring the extent of specular reflection and a parameter of the GGX [42] normal distribution function in the rendering equation. The metalness parameter m and diffuse value k_d can be used to compute the specular term k_s using $k_s = (1-m) \cdot 0.04 + m \cdot k_d$. Furthermore, we use a normal variation k_n in tangent space to enhance the surface lighting effect and introduce additional geometric variations.

We use an MLP Γ as our parameterized material model. Γ is learned to predict spatially varying material parameters, which are subsequently used to render the surface extracted from DMTET. More specifically, for any point $p \in \mathbb{R}^3$ on the surface, we use hash-grid positional encoding [27], and generate the diffuse term k_d, the specular term k_{rm}, and the tangent space normal k_n as:

$$(k_d, k_{rm}, k_n) = \Gamma(\beta(p); \gamma), \tag{6}$$

where β is the positional encoding of p, and γ parameterizes the MLP Γ. The basic rendering equation suggests that each image pixel at a specific viewing direction can be rendered as

$$L(p, \omega) = \int_{\Omega} L_i(p, \omega_i) f(p, \omega_i, \omega)(\omega_i \cdot n_p) \mathrm{d}\omega_i, \tag{7}$$

where L is the rendered pixel color along the direction ω from the surface point p, $\Omega = \{\omega_i : \omega_i \cdot n_p \geq 0\}$ denotes a hemisphere with the incident direction ω_i and surface normal n_p at p, L_i is the incident light that is represented by an off-the-shelf environment map [32], and f is the BRDF determined by the material parameters (k_d, k_{rm}, k_n) predicted by (6). We note that L is the summation of diffuse intensity L_d and specular intensity L_s, and the two terms can be computed as follows:

$$\begin{aligned} L(p, \omega) &= L_d(p) + L_s(p, \omega), \\ L_d(p) &= k_d(1-m) \int_{\Omega} L_i(p, \omega_i)(\omega_i \cdot n_p) \mathrm{d}\omega_i, \\ L_s(p, \omega) &= \int_{\Omega} \frac{DFG}{4(\omega \cdot n_p)(\omega_i \cdot n_p)} L_i(p, \omega_i)(\omega_i \cdot n_p) \mathrm{d}\omega_i, \end{aligned} \tag{8}$$

where F, G, and D represent the Fresnel term, the shadowing-mask term, and the GGX distribution of normal, respectively. Following [28], the hemisphere integration can be calculated using the split-sum method.

By aggregating the rendered pixel colors along the direction ω (i.e., camera pose), we have the rendered image $x = \{L(p, \omega)\}$ that connects with the image encoder of the pre-trained stable diffusion model. We update the parameters γ by computing the gradient of the SDS loss w.r.t. γ:

$$\bigtriangledown_{\gamma} \mathcal{L}_{\text{SDS}}(\phi, x) = \mathbb{E}\left[w(t)(\hat{\epsilon}_{\phi}(z_t^x; y, t) - \epsilon) \frac{\partial x}{\partial \gamma} \frac{\partial z^x}{\partial x} \right]. \tag{9}$$

Notations in (9) are similarly defined as those in (5).

Texturing. Given the trained Γ, we proceed by sampling the generated appearance as 2D texture maps, in accordance with the UV map generated by the xatlas [47]. Note that texture seams would emerge by direct incorporation of the sampled 2D textures into graphics engines (e.g., Blender [10]). We instead employ the UV edge padding technique [9], which involves expanding the boundaries of UV islands and filling empty regions. As illustrated in Fig. 5, this padding technique removes background pixels in the texture map and also removes the seams in the resulting renderings.

Implementation Details. We implement the network Ψ as a three-layer MLP with 32 hidden units, and implement Γ as a two-layer MLP with 32 hidden units. Our method is optimized on 8 Nvidia RTX 3090 GPUs for about 15 minutes for learning Ψ and about 16 minutes for learning Γ, respectively, where we use AdamW optimizer with the respective learning rates of 1×10^{-3} and 1×10^{-2}. For each iteration, we uniformly sample 24 camera poses for the rendering of normal maps and colored images. More details of our implementation are available in the supplemental material. In geometry modeling, we set $\omega(t) = \sigma^2$ during the early phase and then transition to $w(t) = \sigma^2\sqrt{1-\sigma^2}$ as we progress to the later phase. In appearance modeling, we apply $w(t) = \sigma^2\sqrt{1-\sigma^2}$ during the early phase, followed by a shift to $1/\sigma^2$ as we enter the later phase. This approach mitigates the issue related to over-saturated color within the appearance modeling.

5. Experiments

In this section, we present comprehensive experiments to evaluate the efficacy of our proposed method for text-to-3D content creation. We first conduct ablation studies in Section 5.1 that verify the importance of our key design of disentangling geometry and appearance for text-to-3D generation. In Section 5.2, we show the efficacy of our method for the generation of 3D models with PBR materials from arbitrary text prompts, where we also compare with two recent state-of-the-art methods (namely, Magic3D [18] and DreamFusion [33]). In Section 5.3, we present our results

under the setting of user-guided generation and compare them with Latent-NeRF [23]. We finally demonstrate in Section 5.4 that the 3D assets generated by our method are readily compatible with popular graphics engines such as Blender [10], thus facilitating relighting, editing, and physical simulation of the resulting 3D models.

5.1. Ablation studies

We use an example text prompt of "a highly detailed stone bust of Theodoros Kolokotronis" for the ablation studies. Results of alternative settings are given in Fig. 6. As the reference, the first two columns show the geometry and appearance results of our Fantasia3D rendered from the front and back views. To verify the effectiveness of the disentangled design in Fantasia3D, we also conduct experiments as follows: in each iteration, we render shaded images of the mesh extracted from DMTET, and learn to update the parameters of a network responsible for both the geometry and material, using the gradient computed by SDS loss. Results in the second two columns show that such an entangled learning fails to generate plausible results. Previous methods (e.g., DreamFusion [33] and Magic3D [18]) couple the geometry and appearance generation together, following NeRF [25]. Our adoption of the disentangled representation is mainly motivated by the difference of problem nature for generating surface geometry and appearance. In fact, when dealing with finer recovery of surface geometry from multi-view images, methods (e.g., VolSDF [46], nvdiffrec [28], etc) that explicitly take the surface modeling into account triumph; our disentangled representation enjoys the benefit similar to these methods. The disentangled representation also enables us to include the BRDF material representation in the appearance modeling, achieving better photo-realistic rendering by the BRDF physical prior.

To investigate how shape encoding of the normal map plays role in Fantasia3D, we replace the normal map with an image that is shaded on the mesh extracted from DMTET using fixed material parameters; results in the third two columns become weird with twisted geometries. This is indeed one of the key factors that makes the success of Fantasia3D. Our initial hypothesis is that shape information contained in normal and mask images could be beneficial to geometry learning, and as such, we further observe that the value range of normal maps is normalized in (-1, 1), which aligns with the data range required for latent space diffusion; our empirical studies verify our hypothesis. Our hypothesis is further corroborated by observing that the LAION-5B [37] dataset used for training Stable Diffusion contains normals (referring to website for retrieval of normal data in LAION-5B [37]), which allows Stable Diffusion to handle the optimization of normal maps effectively. To deal with rough and coarse geometry in the early stage of learning, we use the concatenated $64 \times 64 \times 4$ (normal, mask) images for better convergence. As the learning progresses, it becomes essential to render the $512 \times 512 \times 3$ high-resolution normal images for capturing finer geometry details, and we choose to use normal images only in the later stage. This strategy strikes an accuracy-efficiency balance throughout the geometry optimization process.

Finally, we replace the full BRDF in Fantasia3D with a simple diffuse color rendering; the results in the last two columns become less realistic and are short of reflection effects when rendered from different views.

5.2. Zero-shot generation

In this section, we evaluate our method for generating 3D assets from solely natural language descriptions (i.e., the setting of zero-shot generation), by comparing with two state-of-the-art methods, namely DreamFusion [33] and Magic3D [18]. Fig. 7 gives the comparative results given the same text prompts. Since DreamFusion and Magic3D do not have released codes, their results are obtained by downloading from their project pages. Comparing our method with Magic3D, we observe that our results are more photorealistic with competitive geometries. We consistently outperform DreamFusion in both appearance and geometry generation. Notably, our method also offers the convenience of easy geometry extraction and editing, as demonstrated in 5.4, which are less obvious from DreamFusion or Magic3D. More of our results are given in the top half of Fig. 2 and Fig. 8. Furthermore, we compare our appearance modeling stage with several mesh stylization methods, namely Text2mesh [24], CLIP-Mesh [14] and Latent-NeRF [23]. Fig. 9 shows that our method excels in generating more realistic appearances, outperforming the other competitors. We present additional results and comparisons in the supplemental materials.

5.3. User-guided generation

In addition to zero-shot generation, our method is flexible to accept a customized 3D model as the initialization, alternative to a 3D ellipsoid, thereby facilitating user-guided asset generation. As shown in the lower half of Fig. 2, our method is able to generate rich details in both the geometry and appearance when provided with low-quality 3D models for initialization. The three meshes used in the experiments are from Text2Mesh [24], Latent-NeRF [23], and the creation of Stable DreamFusion [41], respectively. We also compare with the state-of-the-art approach of Latent-NeRF [23] under this user-guided generation setting; results are given in Fig. 10. Our method outperforms Latent-NeRF [23] in both the geometry and texture generation when given the same input meshes and text prompts.

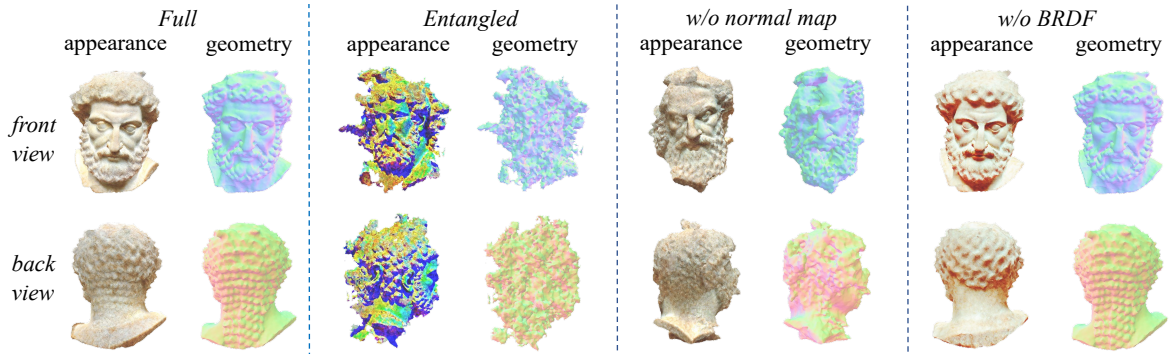

Figure 6. **Ablation studies of our method.** The text prompt is "a highly detailed stone bust of Theodoros Kolokotronis". Please refer to Section 5.1 for specific settings of individual columns. Please refer to the video results in the supplemental materials for better comparisons.

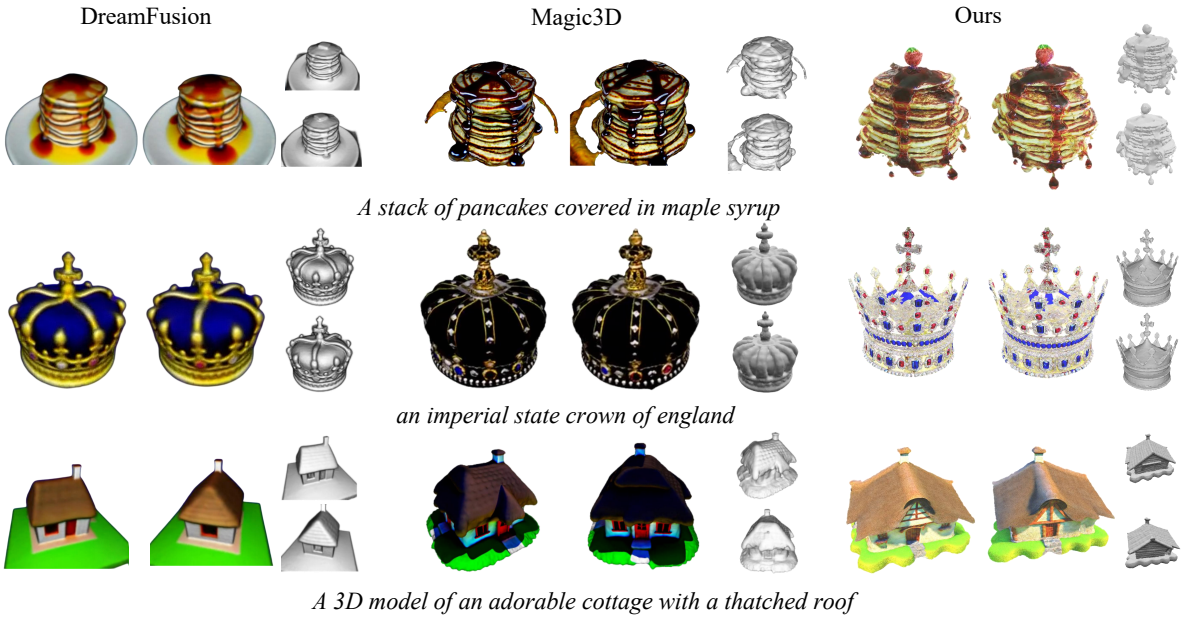

Figure 7. **Comparison of zero-shot generation.** Since DreamFusion and Magic3D do not have released codes, their results are obtained by downloading from their project pages. More results and comparisons are available in the supplemental materials.

Figure 8. **Geometries beyond genus-zero ones.** DMTET can deform to any topologies, which enables Fantasia3D to generate complex geometries, including those beyond genus-zero ones.

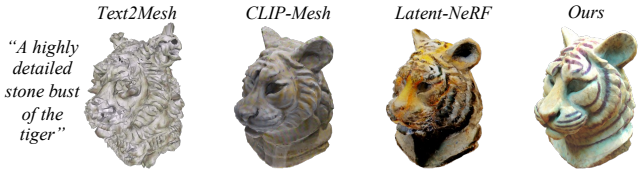

Figure 9. **Comparison of Texturing.** We compare the appearance stage of Fantasia3D with three text-driven texturing methods, using the geometry generated by the geometry stage of Fantasia3D.

5.4. Scene editing and simulation

Given the disentangled design, our method produces high-quality generation of both the surface and appearance, and is compatible with popular graphics engines for scene editing and physical simulation. In Figure 1, we import into Blender a stone statue generated by our method from the text prompt of "a highly detailed stone bust of Theodoros Kolokotronis", where soft body and cloth simulations are performed along with material editing. Given the high qual-

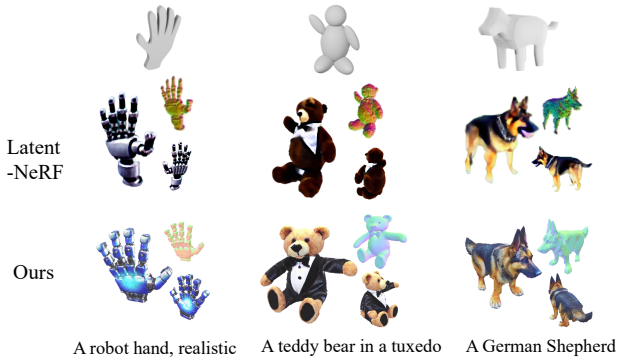

Figure 10. **Comparison of user-guided generation.** The top row shows the input meshes provided by users, the bottom row gives the input text prompts, and the middle two rows show the results from the comparative methods.

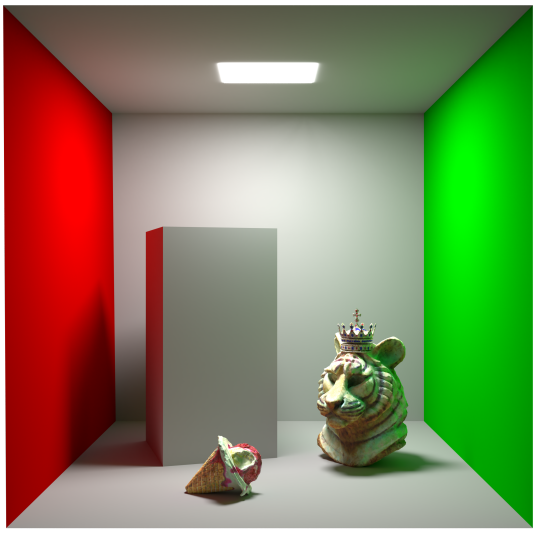

Figure 11. **Scene Editing.** Three generated objects, namely crown, tiger, and ice cream, are imported into the Cornell Box scene. The scene is then rendered using the Cycles path tracer in Blender, producing natural shadows and reflectance effects.

Figure 12. **Relighting.** Our generated Iron Man model is relit using different lighting setups in Blender, producing diverse reflectance effects on the armor.

ity of the generated surface geometry (e.g., no holes on the surface), the simulations are of high-level physical accuracy, as shown in the accompanying supplemental video. Moreover, we showcase the ability to modify the material of the statue by replacing it with another wood material downloaded from the Internet [32], which poses a challenge for comparative methods such as DreamFusion [33]. Additionally, in Fig. 11, by importing generated ice cream, tiger, and crown into the Cornell Box, we demonstrate the plausible physical interaction between our generated results and the scene, with natural shadows being cast. Finally, Fig. 12 illustrates the replacement of the HDR environment map to produce diverse lighting and corresponding reflectance effects on the generated iron man.

6. Limitations

While Fantasia3D demonstrates promising advancements in the realm of generating photorealistic 3D assets from text prompts, several limitations remain. For instance, while our method successfully produces loose visual effects, it remains a significant challenge to generate corresponding loose geometries, such as hair, fur, and grass, solely based on text prompts. Additionally, our method primarily emphasizes object generation, thereby lacking the capacity to generate complete scenes with background from text prompts. Consequently, our future research endeavors will be dedicated to addressing these limitations by focusing on the generation of complete scenes and intricate loose geometries.

7. Conclusion

In this paper, we present Fantasia3D, a new method for automatic text-to-3D generation. Fantasia3D uses disentangled modeling and learning of geometry and appearance, and is able to generate both the fine surface and rich material/texture. Fantasia3D is based on the hybrid scene representation of DMTET. For geometry learning, we propose to encode a rendered normal map, and use shape encoding of the normal as the input of the pre-trained, stable diffusion model. For appearance modeling, we introduce the spatially varying BRDF into the text-to-3D task, thus enabling material learning that supports photorealistic rendering of the learned surface. Expect for text prompts, our method can be triggered with a customized 3D shape as well; this is flexible for users to better control what content is to be generated. Our method is also convenient to support relighting, editing, and physical simulation of the generated 3D assets. Our method is based on pre-trained image diffusion models (i.e., the stable diffusion). In future research, we are interested in learning 3D diffusion directly from the large language models.

Acknowledgements. This work is supported in part by Program for Guangdong Introducing Innovative and Entrepreneurial Teams (No.: 2017ZT07X183) and Guangdong R&D key project of China (No.: 2019B010155001).

References

[1] Miika Aittala, Timo Aila, and Jaakko Lehtinen. Reflectance modeling by neural texture synthesis. *ACM Transactions on Graphics (TOG)*, 35(4):1–13, 2016.

[2] Miika Aittala, Tim Weyrich, and Jaakko Lehtinen. Practical svbrdf capture in the frequency domain. *ACM SIGGRAPH*, 32(4):110–1, 2013.

[3] Yogesh Balaji, Seungjun Nah, Xun Huang, Arash Vahdat, Jiaming Song, Karsten Kreis, Miika Aittala, Timo Aila, Samuli Laine, Bryan Catanzaro, Tero Karras, and Ming-Yu Liu. ediff-i: Text-to-image diffusion models with ensemble of expert denoisers. *arXiv preprint arXiv:2211.01324*, 2022.

[4] Jonathan T. Barron, Ben Mildenhall, Matthew Tancik, Peter Hedman, Ricardo Martin-Brualla, and Pratul P. Srinivasan. Mip-nerf: A multiscale representation for anti-aliasing neural radiance fields. In *Proceedings of the IEEE/CVF International Conference on Computer Vision (ICCV)*, pages 5855–5864, October 2021.

[5] Sai Bi, Zexiang Xu, Pratul Srinivasan, Ben Mildenhall, Kalyan Sunkavalli, Miloš Hašan, Yannick Hold-Geoffroy, David Kriegman, and Ravi Ramamoorthi. Neural reflectance fields for appearance acquisition. *arXiv preprint arXiv:2008.03824*, 2020.

[6] Wenzheng Chen, Huan Ling, Jun Gao, Edward Smith, Jaakko Lehtinen, Alec Jacobson, and Sanja Fidler. Learning to predict 3d objects with an interpolation-based differentiable renderer. *Advances in Neural Information Processing Systems (NeurIPS)*, 32, 2019.

[7] Wenzheng Chen, Joey Litalien, Jun Gao, Zian Wang, Clement Fuji Tsang, Sameh Khamis, Or Litany, and Sanja Fidler. Dib-r++: learning to predict lighting and material with a hybrid differentiable renderer. *Advances in Neural Information Processing Systems (NeurIPS)*, 34:22834–22848, 2021.

[8] Yongwei Chen, Rui Chen, Jiabao Lei, Yabin Zhang, and Kui Jia. Tango: Text-driven photorealistic and robust 3d stylization via lighting decomposition. *Advances in Neural Information Processing Systems (NeurIPS)*, 2022.

[9] Clarisse. UV edge padding. `https://clarissewiki.com/4.0/uv_edge_padding.html`.

[10] Blender Online Community. *Blender - a 3D modelling and rendering package*. Blender Foundation, Stichting Blender Foundation, Amsterdam, 2018.

[11] Valentin Deschaintre, Miika Aittala, Fredo Durand, George Drettakis, and Adrien Bousseau. Single-image svbrdf capture with a rendering-aware deep network. *ACM Transactions on Graphics (TOG)*, 37(4):1–15, 2018.

[12] Duan Gao, Xiao Li, Yue Dong, Pieter Peers, Kun Xu, and Xin Tong. Deep inverse rendering for high-resolution svbrdf estimation from an arbitrary number of images. *ACM Transactions on Graphics (TOG)*, 38(4):134–1, 2019.

[13] Ajay Jain, Ben Mildenhall, Jonathan T Barron, Pieter Abbeel, and Ben Poole. Zero-shot text-guided object generation with dream fields. In *Proceedings of the IEEE/CVF Conference on Computer Vision and Pattern Recognition (CVPR)*, pages 867–876, 2022.

[14] Nasir Mohammad Khalid, Tianhao Xie, Eugene Belilovsky, and Popa Tiberiu. Clip-mesh: Generating textured meshes from text using pretrained image-text models. *ACM SIGGRAPH*, 2022.

[15] Matthias Labschütz, Katharina Krösl, Mariebeth Aquino, Florian Grashäftl, and Stephanie Kohl. Content creation for a 3D game with maya and unity 3D. *Institute of Computer Graphics and Algorithms, Vienna University of Technology*, 6:124, 2011.

[16] Samuli Laine, Janne Hellsten, Tero Karras, Yeongho Seol, Jaakko Lehtinen, and Timo Aila. Modular primitives for high-performance differentiable rendering. *ACM Transactions on Graphics (TOG)*, 39(6), 2020.

[17] Muheng Li, Yueqi Duan, Jie Zhou, and Jiwen Lu. Diffusion-sdf: Text-to-shape via voxelized diffusion. *arXiv preprint arXiv:2212.03293*, 2022.

[18] Chen-Hsuan Lin, Jun Gao, Luming Tang, Towaki Takikawa, Xiaohui Zeng, Xun Huang, Karsten Kreis, Sanja Fidler, Ming-Yu Liu, and Tsung-Yi Lin. Magic3D: High-resolution text-to-3D content creation. *arXiv preprint arXiv:2211.10440*, 2022.

[19] Shichen Liu, Tianye Li, Weikai Chen, and Hao Li. Soft rasterizer: A differentiable renderer for image-based 3d reasoning. In *Proceedings of the IEEE/CVF International Conference on Computer Vision (ICCV)*, pages 7708–7717, 2019.

[20] William E Lorensen and Harvey E Cline. Marching cubes: A high resolution 3D surface construction algorithm. *ACM SIGGRAPH*, 21(4):163–169, 1987.

[21] Stephen McAuley, Stephen Hill, Naty Hoffman, Yoshiharu Gotanda, Brian Smits, Brent Burley, and Adam Martinez. Practical physically-based shading in film and game production. In *ACM SIGGRAPH 2012 Courses*, pages 1–7. 2012.

[22] Lars Mescheder, Michael Oechsle, Michael Niemeyer, Sebastian Nowozin, and Andreas Geiger. Occupancy networks: Learning 3D reconstruction in function space. In *Proceedings of the IEEE/CVF Conference on Computer Vision and Pattern Recognition (CVPR)*, pages 4460–4470, 2019.

[23] Gal Metzer, Elad Richardson, Or Patashnik, Raja Giryes, and Daniel Cohen-Or. Latent-nerf for shape-guided generation of 3D shapes and textures. *arXiv preprint arXiv:2211.07600*, 2022.

[24] Oscar Michel, Roi Bar-On, Richard Liu, Sagie Benaim, and Rana Hanocka. Text2mesh: Text-driven neural stylization for meshes. *Proceedings of the IEEE/CVF Conference on Computer Vision and Pattern Recognition (CVPR)*, 2022.

[25] Ben Mildenhall, Pratul P Srinivasan, Matthew Tancik, Jonathan T Barron, Ravi Ramamoorthi, and Ren Ng. Nerf: Representing scenes as neural radiance fields for view synthesis. *Proceedings of the European Conference on Computer Vision (ECCV)*, 2020.

[26] Alexander Mordvintsev, Nicola Pezzotti, Ludwig Schubert, and Chris Olah. Differentiable image parameterizations. *Distill*, 3(7):e12, 2018.

[27] Thomas Müller, Alex Evans, Christoph Schied, and Alexander Keller. Instant neural graphics primitives with a multiresolution hash encoding. *ACM Transactions on Graphics (TOG)*, 41(4):1–15, 2022.

[28] Jacob Munkberg, Jon Hasselgren, Tianchang Shen, Jun Gao, Wenzheng Chen, Alex Evans, Thomas Müller, and Sanja Fidler. Extracting triangular 3D models, materials, and lighting from images. In *Proceedings of the IEEE/CVF Conference on Computer Vision and Pattern Recognition (CVPR)*, pages 8280–8290, 2022.

[29] Gimin Nam, Mariem Khlifi, Andrew Rodriguez, Alberto Tono, Linqi Zhou, and Paul Guerrero. 3D-LDM: Neural implicit 3D shape generation with latent diffusion models. *arXiv preprint arXiv:2212.00842*, 2022.

[30] Alex Nichol, Prafulla Dhariwal, Aditya Ramesh, Pranav Shyam, Pamela Mishkin, Bob McGrew, Ilya Sutskever, and Mark Chen. Glide: Towards photorealistic image generation and editing with text-guided diffusion models. *Proceedings of Machine Learning Research (PMLR)*, 2021.

[31] Jeong Joon Park, Peter Florence, Julian Straub, Richard Newcombe, and Steven Lovegrove. Deepsdf: Learning continuous signed distance functions for shape representation. In *Proceedings of the IEEE/CVF Conference on Computer Vision and Pattern Recognition (CVPR)*, pages 165–174, 2019.

[32] Poliigon. Poliigon. `https://www.poliigon.com`.

[33] Ben Poole, Ajay Jain, Jonathan T Barron, and Ben Mildenhall. Dreamfusion: Text-to-3d using 2d diffusion. *International Conference on Learning Representations (ICLR)*, 2023.

[34] Aditya Ramesh, Prafulla Dhariwal, Alex Nichol, Casey Chu, and Mark Chen. Hierarchical text-conditional image generation with clip latents. *arXiv preprint arXiv:2204.06125*, 2022.

[35] Robin Rombach, Andreas Blattmann, Dominik Lorenz, Patrick Esser, and Björn Ommer. High-resolution image synthesis with latent diffusion models. In *Proceedings of the IEEE/CVF Conference on Computer Vision and Pattern Recognition (CVPR)*, pages 10684–10695, 2022.

[36] Chitwan Saharia, William Chan, Saurabh Saxena, Lala Li, Jay Whang, Emily Denton, Seyed Kamyar Seyed Ghasemipour, Burcu Karagol Ayan, S Sara Mahdavi, Rapha Gontijo Lopes, et al. Photorealistic text-to-image diffusion models with deep language understanding. *Advances in Neural Information Processing Systems (NeurIPS)*, 2022.

[37] Christoph Schuhmann, Romain Beaumont, Richard Vencu, Cade Gordon, Ross Wightman, Mehdi Cherti, Theo Coombes, Aarush Katta, Clayton Mullis, Mitchell Wortsman, et al. Laion-5b: An open large-scale dataset for training next generation image-text models. *Advances in Neural Information Processing Systems (NeurIPS)*, 2022.

[38] Tianchang Shen, Jun Gao, Kangxue Yin, Ming-Yu Liu, and Sanja Fidler. Deep marching tetrahedra: a hybrid representation for high-resolution 3D shape synthesis. In *Advances in Neural Information Processing Systems (NeurIPS)*, 2021.

[39] J Ryan Shue, Eric Ryan Chan, Ryan Po, Zachary Ankner, Jiajun Wu, and Gordon Wetzstein. 3D neural field generation using triplane diffusion. *arXiv preprint arXiv:2211.16677*, 2022.

[40] Stability.AI. Stable diffusion. `https://stability.ai/blog/stable-diffusion-public-release`.

[41] Jiaxiang Tang. Stable dreamfusion. `https://github.com/ashawkey/stable-dreamfusion`.

[42] Bruce Walter, Stephen R Marschner, Hongsong Li, and Kenneth E Torrance. Microfacet models for refraction through rough surfaces. In *Proceedings of the 18th Eurographics conference on Rendering Techniques*, pages 195–206, 2007.

[43] Peng Wang, Lingjie Liu, Yuan Liu, Christian Theobalt, Taku Komura, and Wenping Wang. Neus: Learning neural implicit surfaces by volume rendering for multi-view reconstruction. *Advances in Neural Information Processing Systems (NeurIPS)*, 2021.

[44] Tengfei Wang, Bo Zhang, Ting Zhang, Shuyang Gu, Jianmin Bao, Tadas Baltrusaitis, Jingjing Shen, Dong Chen, Fang Wen, Qifeng Chen, et al. Rodin: A generative model for sculpting 3d digital avatars using diffusion. *Proceedings of the IEEE/CVF Conference on Computer Vision and Pattern Recognition (CVPR)*, 2023.

[45] Hongzhi Wu, Julie Dorsey, and Holly Rushmeier. A sparse parametric mixture model for btf compression, editing and rendering. In *Computer Graphics Forum (Comput Graph Forum)*, volume 30, pages 465–473. Wiley Online Library, 2011.

[46] Lior Yariv, Jiatao Gu, Yoni Kasten, and Yaron Lipman. Volume rendering of neural implicit surfaces. In *Advances in Neural Information Processing Systems (NeurIPS)*, 2021.

[47] Jonathan Young. xatlas. `https://github.com/jpcy/xatlas.git`, 2021.

[48] Yuxuan Zhang, Wenzheng Chen, Huan Ling, Jun Gao, Yinan Zhang, Antonio Torralba, and Sanja Fidler. Image gans meet differentiable rendering for inverse graphics and interpretable 3d neural rendering. *International Conference on Learning Representations (ICLR)*, 2020.

[49] Linqi Zhou, Yilun Du, and Jiajun Wu. 3d shape generation and completion through point-voxel diffusion. In *Proceedings of the IEEE/CVF International Conference on Computer Vision (ICCV)*, pages 5826–5835, 2021.